Supplementary Data

MAZ induces *MYB* expression during the exit from quiescence via the E2F site in the *MYB* promoter.

[1,8]Josué Álvaro-Blanco, [2,8]Katia Urso, [1,8]Yuri Chiodo, [1]Carla Martín-Cortázar, [1]Omar Kourani, [2,3,4]Pablo Gómez-del Arco, [1]María Rodríguez-Martínez, [5]Esther Calonge, [5]José Alcamí, [2,4]Juan Miguel Redondo, [6,7]Teresa Iglesias, and [1,4,9]Miguel R. Campanero.

A

Observed	Mr(expt)	Mr(calc)		Start		End	Peptide
916.2865	915.2792	915.4562		290	-	296	R.DVYHLNR.H
999.4016	998.3943	998.5185		427	-	435	K.GFTTAAYLR.I
1228.4810	1227.4737	1227.6360		358	-	367	R.QVHSTERPFK.C
1551.5127	1550.5054	1550.7702		345	-	357	K.SFSRPDHLNSHVR.Q
1801.4795	1800.4722	1800.8148		412	-	426	K.VHSQGPHHVCELCNK.G
1953.4711	1952.4638	1952.8370		328	-	344	R.SHDGAVHKPYNCSHCGK.S
2131.5514	2130.5442	2130.9575		299	-	315	K.LSHSDEKPYQCPVCQQR.F

B

```
MAZ-1|P56270-1   MFPVFPCTLLAPPFPVLGLDSRGVGGLMNSFPPPQGHAQNPLQVGAELQSRFFASQGCAQ 60
MAZ-2|P56270-2|  MFPVFPCTLLAPPFPVLGLDSRGVGGLMNSFPPPQGHAQNPLQVGAELQSRFFASQGCAQ 60
MAZ-3|P56270-3|  ------------------MDPS-----NWSSFIFQGHAQNPLQVGAELQSRFFASQGCAQ 37
MAZ-2s|Q8IUI2|   ------------------------------------------------------------
                  ****************************

MAZ-1|P56270-1|  SPFQAAPAPPPTPQAPAAEPLQVDLLPVLAAAQESAAAAAAAAAAAAAVAAAPPAPAAAS 120
MAZ-2|P56270-2|  SPFQAAPAPPPTPQAPAAEPLQVDLLPVLAAAQESAAAAAAAAAAAAAVAAAPPAPAAAS 120
MAZ-3|P56270-3|  SPFQAAPAPPPTPQAPAAEPLQVDLLPVLAAAQESAAAAAAAAAAAAAVAAAPPAPAAAS 97
MAZ-2s|Q8IUI2|   ------------------------------------------------------------

MAZ-1|P56270-1|  TVDTAALKQPPAPPPPPPVSAPAAEAAPPASAATIAAAAATAVVAPTSTVAVAPVASAL 180
MAZ-2|P56270-2|  TVDTAALKQPPAPPPPPPVSAPAAEAAPPASAATIAAAAATAVVAPTSTVAVAPVASAL 180
MAZ-3|P56270-3|  TVDTAALKQPPAPPPPPPVSAPAAEAAPPASAATIAAAAATAVVAPTSTVAVAPVASAL 157
MAZ-2s|Q8IUI2|   ------------------------------------------------------------

MAZ-1|P56270-1|  EKKTKSKGPYICALCAKEFKNGYNLRRHEAIHTGAKAGRVPSGAMKMPTMVPLSLLSVPQ 240
MAZ-2|P56270-2|  EKKTKSKGPYICALCAKEFKNGYNLRRHEAIHTGAKAGRVPSGAMKMPTMVPLSLLSVPQ 240
MAZ-3|P56270-3|  EKKTKSKGPYICALCAKEFKNGYNLRRHEAIHTGAKAGRVPSGAMKMPTMVPLSLLSVPQ 217
MAZ-2s|Q8IUI2|   ------------------------------------------------MVPLSLLSVPQ 11

MAZ-1|P56270-1|  LSGAGGGGGEAGAGGGAAAVAAGGVVTTTASGKRIRKNHACEMCGKAFRDVYHLNRHKLS 300
MAZ-2|P56270-2|  LSGAGGGGGEAGAGGGAAAVAAGGVVTTTASGKRIRKNHACEMCGKAFRDVYHLNRHKLS 300
MAZ-3|P56270-3|  LSGAGGGGGEAGAGGGAAAVAAGGVVTTTASGKRIRKNHACEMCGKAFRDVYHLNRHKLS 277
MAZ-2s|Q8IUI2|   LSGAGGGGGEAGAGGGAAAVAAGGVVTTTASGKRIRKNHACEMCGKAFRDVYHLNRHKLS 71

MAZ-1|P56270-1|  HSDEKPYQCPVCQQRFKRKDRMSYHVRSHDGAVHKPYNCSHCGKSFSRPDHLNSHVRQVH 360
MAZ-2|P56270-2|  HSDEKPYQCPVCQQRFKRKDRMSYHVRSHDGAVHKPYNCSHCGKSFSRPDHLNSHVRQVH 360
MAZ-3|P56270-3|  HSDEKPYQCPVCQQRFKRKDRMSYHVRSHDGAVHKPYNCSHCGKSFSRPDHLNSHVRQVH 337
MAZ-2s|Q8IUI2|   HSDEKPYQCPVCQQRFKRKDRMSYHVRSHDGAVHKPYNCSHCGKSFSRPDHLNSHVRQVH 131

MAZ-1|P56270-1|  STERPFKCEKCEAAFATKDRLRAHTVRHEEKVPCHVCGKMLSSAYISDHMKVHSQGPHHV 420
MAZ-2|P56270-2|  STERPFKCEKCEAAFATKDRLRAHTVRHEEKVPCHVCGKMLSSAYISDHMKVHSQGPHHV 420
MAZ-3|P56270-3|  STERPFKCEKCEAAFATKDRLRAHTVRHEEKVPCHVCGKMLSSAYISDHMKVHSQGPHHV 397
MAZ-2s|Q8IUI2|   STERPFKCEKCEAAFATKDRLRAHTVRHEEKVPCHVCGKMLSSAYISDHMKVHSQGPHHV 191

MAZ-1|P56270-1|  CELCNKGTGEVCPMAAAAAAAAAAAA-----------AAVAAPPTAVGSLS---GAEGV 465
MAZ-2|P56270-2|  CELCNKGPTTAAYLRIHAVKDHGLQAPRADRILCKLCSVHCKTPAQLAGHMQTHLGGAAP 480
MAZ-3|P56270-3|  CELCNKGTGEVCPMAAAAAAAAAAAA-----------AAVAAPPTAVGSLS---GAEGV 442
MAZ-2s|Q8IUI2|   CELCNKGPTTAAYLRIHAVKDHGLQAPRADRILCKLCSVHCKTPAQLAGHMQTHLGGAAP 251
                  ************************************************

MAZ-1|P56270-1|  PVSSQPLPSQPW- 477
MAZ-2|P56270-2|  PVPGDAPQPQPTC 493
MAZ-3|P56270-3|  PVSSQPLPSQPW- 454
MAZ-2s|Q8IUI2|   PVPGDAPQPQPTC 264
                 *************
```

Figure S1. MAZ peptides identified by mass spectrometry analysis. (**A**) Experimentally observed m/z values, monoisotopic mass (Mr expt), and theoretically calculated (Mr calc) values of tryptic peptides commonly detected in LC-MS/MS analysis of 2 independent purification experiments. The start and end position of these peptides in MAZ-1 and their sequence is indicated. (**B**) Alignment of indicated MAZ isoforms. Asterisks denote the position of isoform-specific amino acids. Uniprot accession numbers are indicated for each isoform. Gray box, MAZ-3-specific sequence; yellow box, carboxyl-terminal end common to MAZ-1 and MAZ-3; green box, carboxy-terminal end common to MAZ-2 and MAZ-2s. Peptides identified by mass spectrometry are labeled in bold-red.

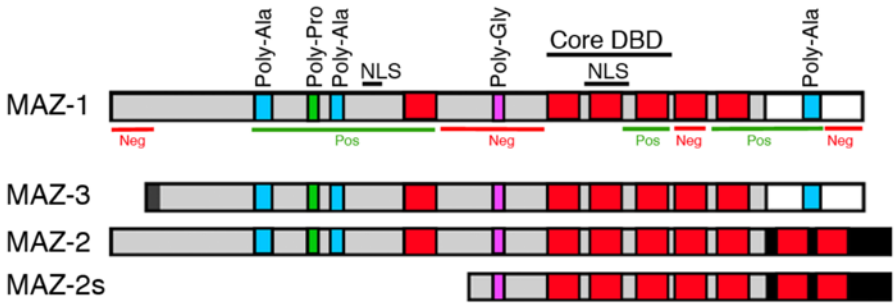

Figure S2. Diagram of MAZ isoforms. The presence of zinc fingers (red boxes), poly-Ala tracts, a poly-Gly and a poly-Pro tract, nuclear localization signals (NLS), a DNA-binding domain (DBD), and regions that positively (Pos) or negatively (Neg) regulate transcription is indicated, as previously reported for MAZ-1 (Reference 27).

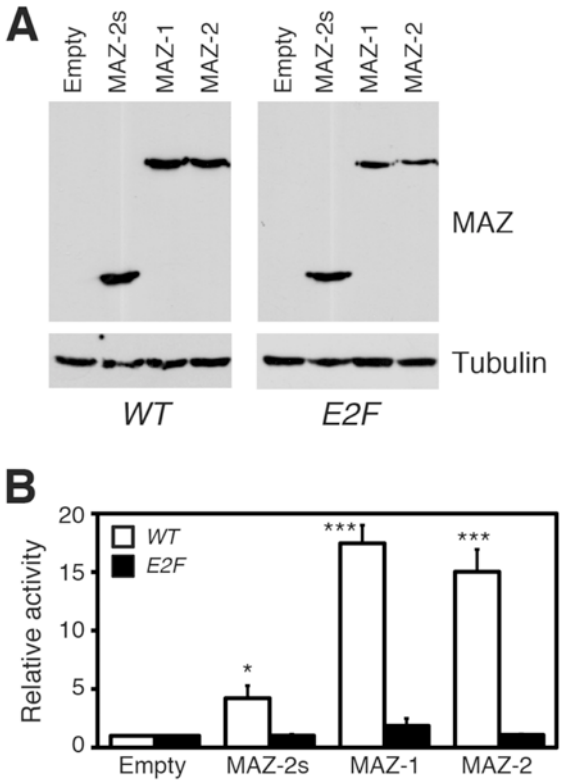

Figure S3. MAZ-2s activates transcription less efficiently than MAZ-1 or MAZ-2. The indicated *WT* and *E2F 2xE2F/MAZ-Luc* plasmids were cotransfected with *pRL-null* in asynchronously growing Saos-2 cells in the presence of plasmids encoding MAZ-2s, MAZ-1, MAZ-2, or empty vector. Forty hours later, cell extracts were prepared for immunoblotting or for firefly and renilla luciferase analysis. (**A**) Immunoblot analysis employing the anti-MAZ MAZ-123 antibody and anti-Tubulin. (**B**) Firefly luciferase values were normalized for renilla activity. Luciferase activity is shown relative to that in the presence of the empty vector (mean±SEM; n=3). *p<0.05 and ***p<0.001 vs empty; two-way ANOVA with Bonferroni post-test.

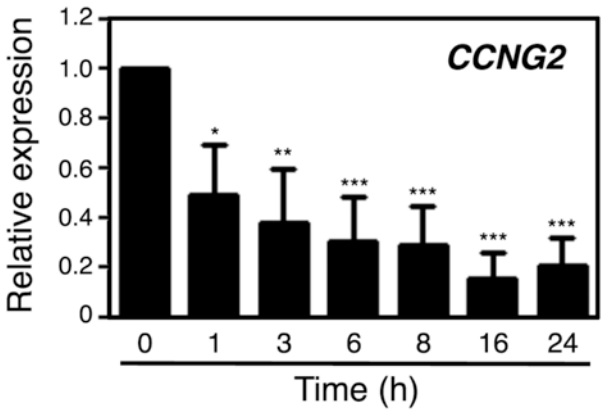

Figure S4. *CCNG2* levels decrease during the exit from quiescence. IL2-starved lymphocytes were stimulated to re-enter the cell cycle for the indicated periods of time. RT-qPCR analysis of *CCNG2* mRNA levels were determined in these cells by RT-qPCR and normalized to *GUSB* expression. Data are shown as means±SEM (n=3) relative to 0h. *p<0.05, **p<0.01, ***p<0.001 vs 0h; One-way ANOVA with Bonferroni post-test.

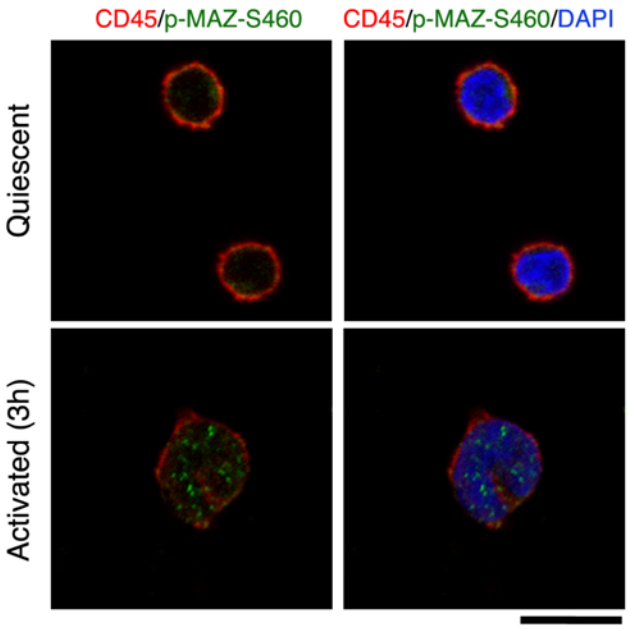

Figure S5. MAZ is activated shortly after the exit from quiescence. IL2-starved lymphocytes were stimulated to re-enter the cell cycle for 3h. Representative confocal microscopy images of the plasma membrane protein CD45 (red), p-MAZ S460 and DAPI staining in quiescent lymphocytes and in cells stimulated to re-enter the cell cycle for 3h. Bar, 10 µm.

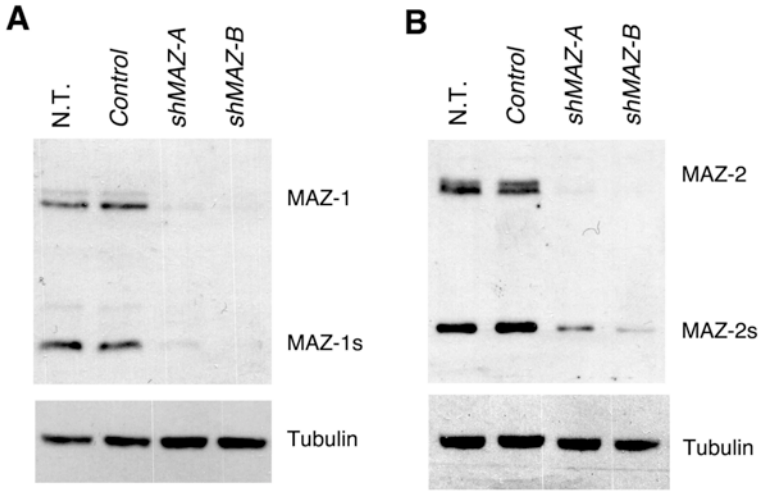

Figure S6. *MAZ*-specific shRNAs readily knockdown *MAZ* expression. Jurkat T cells were transduced with lentivirus encoding *MAZ*-specific shRNA (*shMAZ-A*, *shMAZ-B*) or a control shRNA. MAZ levels were analyzed by immunoblot in extracts from these cells and in non-transduced cells (N.T.) employing (**A**) M-13 or (**B**) M-2 anti-MAZ antibodies. Tubulin was used as a loading control.